ELSEVIER

Journal of Chromatography A, 916 (2001) 255–263

JOURNAL OF CHROMATOGRAPHY A

www.elsevier.com/locate/chroma

Chemometric modeling of neurotransmitter amino acid separation in normal and reversed migration micellar electrokinetic chromatography

Hong Wan, Marcus Öhman, Lars G. Blomberg*

Department of Chemistry, Karlstad University, SE-651 88 Karlstad, Sweden

Abstract

A chemometric experimental design has been applied for the optimization of neurotransmitter amino acid separation in capillary electrophoresis. The optimizations were carried out for normal micellar electrokinetic chromatography (N-MEKC) and reversed migration micellar electrokinetic chromatography (RM-MEKC). In order to optimize three separation factors and study the interaction between factors, a response function was optimized via searching its optimum (minimum/maximum). For this purpose a central composite design with multivariate linear regression (MLR) analysis was utilized. Modeling with good regression coefficients from the MLR adequately described the interaction of factors such as background electrolyte and sodium dodecylsulfate concentrations which had a large impact on selectivity and migration behaviors. Similar optimal conditions regarding resolution and number of theoretical plates but different retention behaviors as a function of background electrolyte and micellar concentrations were observed for N-MEKC and RM-MEKC. Improved overall performance from the RM-MEKC separation of five neurotransmitter acids, superior to N-MEKC, is demonstrated in terms of repeatability, peak symmetry, sensitivity, and in particular, impurity determination in an overloaded separation system.

Keywords: Chemometrics; Central composite design; Mathematical modelling; Electrokinetic chromatography; Experimental design; Optimization; Amino acids; Neurotransmitters

1. Introduction

Micellar electrokinetic chromatography (MEKC) is one of the most widely used CE separation modes and it has been extensively investigated and successfully applied for the separation of various compounds. Recently, Quirino and Terabe have demonstrated an additional advantage of MEKC, the possibility to increase the detection sensitivity for neutral and hydrophobic compounds using MEKC mode combining with stacking and a so-called sweeping technique [1–7]. Further, they presented an example of separation of alkylphenyl ketones in uncoated capillaries by reversed migration micellar electrokinetic chromatography (RM-MEKC) where elution order was reversed as compared to normal micellar electrokinetic chromatography (N-MEKC) [8]. The N-MEKC and RM-MEKC separations were, however, performed in different background electrolytes, thus, a true comparison of the two techniques regarding their optimal conditions and separation performances could not be done. From a theoretical point of view, it was concluded that resolution in RM-MEKC is better than in N-MEKC [8]. MEKC in

*Corresponding author. Tel.: +46-54-700-1530; fax: +46-54-700-1424.

E-mail address: lars.blomberg@kau.se (L.G. Blomberg).

0021-9673/01/$ – see front matter
PII: S0021-9673(00)01174-2

coated capillaries has been reported before [9–14]. Janini et al. called this technique reversed flow MEKC (RF-MEKC) [12]. However, these authors performed micellar separations under acidic conditions on coated capillaries. Since there was no EOF, the term reversed flow MEKC seems to be somewhat misleading. So far, the migration behaviors in the RM-MEKC mode regarding the optimal conditions have not been studied in detail.

Many methods have been applied for optimization of separation variables in chromatography and capillary electrophoresis [15–22]. In the present work we wanted to obtain optimization, response surface and interaction studies. A comparison of the performance of six different experimental designs including factorial, fractional factorial, central composite, Plakett–Burman, overlapping resolution mapping and Simplex has been given by Altria et al. [21]. In this comparison central composite design (CCD) gave the performance, including variable interactions, that we required, and that was at the lowest number of experiments. The data were treated by multiple linear regression (MLR). MLR is a very useful method for the analysis of data for experimental design. MLR fits a model to the data such that the sum of the squared *y*-residuals is minimized. The outcome is a model consisting of regression coefficients, which are utilized to interpret the influence of the factors. Further, there is a clear cause–effect relationship (both *x* and *y* variables are internally independent) [23,24].

Capillary electrophoretic separations of neurotransmitter amino acids using various separation modes and detection techniques have been presented in a number of publications [25–31]. In this work, we utilized five primary neurotransmitter amino acids as probes to compare their separation in N-MEKC and RM-MEKC. Different retention behaviors in these two separation modes were illustrated. The benefit of reversing elution order to facilitate impurity determination in an overloaded system was also demonstrated.

2. Experimental

2.1. Chemicals and reagents

Neurotransmitter amino acid standards, DL-alanine (Ala), DL-aspartic acid (Asp), DL-glutamic acid (Glu), glycine (Gly), γ-amino-*n*-butyric acid (GABA), were obtained from Sigma (St. Louis, MO, USA). The derivatization reagent, 9-fluorenylmethyl chloroformate (FMOC) and sodium dodecylsulfate (SDS) were from Fluka (Buchs, Switzerland). Boric acid and tris(hydroxymethyl)aminomethane (Tris) were from Aldrich (Gillingham, UK). Polypropylene filters were from Arbor Technologies (Ann Arbor, MI, USA). Other chemicals used in this work were of analytical grade.

2.2. Apparatus and separation conditions

MEKC separations were performed on a HP^{3D} CE capillary electrophoresis instrument (Hewlett-Packard). In the N-MEKC mode on uncoated capillaries, a normal polarity, e.g., positive high voltage was applied. In the RM-MEKC separation on coated capillaries, a reversed polarity (negative high voltage) was applied. Detection was by direct UV at 214 nm. The diode array detector was scanned from 190 to 400 nm to confirm peak identification. Experimental designs and multivariate analysis for the optimization and modeling were done using two computer programs, Modde 5.0 (Umetrics, Umeå, Sweden) and Codex program (Sum IT System, Sollentuna, Sweden).

Fused-silica capillaries, 50 μm I.D., were obtained from Polymicro Technologies (Phoenix, AZ, USA). Coating was with polydimethylacrylamide [32]. The coated capillaries were stable under the conditions applied in this work. New uncoated capillaries were first pre-treated by flushing with 0.4 *M* NaOH for 30–60 min and then with water for 10 min. Between runs, the capillary was subsequently flushed with 0.2 *M* NaOH for 2 min, water for 1 min and running buffer for 3 min. Newly coated capillaries were flushed with Milli-Q water for 10 min before starting separation and then flushed only with water and buffer between runs. Samples were normally introduced by pressure (50 mbar, 10 s). Other separation conditions are given in the corresponding figure legends and tables.

2.3. Preparation of samples and buffers

Derivatization of amino acids with FMOC was the same as described before [33]. Each concentration of

mixed FMOC-amino acids was about 200 μ*M*. In order to be able to detect impurities a more highly concentrated sample (1.0 m*M*) was injected. Borate–NaOH (pH 8.60) buffer used as background electrolyte (BGE) was prepared with purified water which gave a conductivity of 18.2 MΩ cm from Millipore Milli-Q plus (Millipore, Molsheim, France). After degassing and filtering using a 0.45 μm filters, the buffers could be used for more than 2 weeks when being stored at 4°C.

3. Results and discussion

The amino acids were derivatized with FMOC and therefore a relatively high pH was required for their separation. Although not optimized, a pH of 8.60 was selected for this work. To perform RM-MEKC, the capillaries have to be coated however the commonly used polyacrylamide coating is not stable at pH 8.60. Therefore, we used a new type of permanent coating consisting of polydimethylacrylamide [32].

According to Terabe et al. [34], resolution in normal MEKC can be written as:

$$R_{s_{\text{N-MEKC}}} = \frac{\sqrt{N}}{4}\cdot\left(\frac{\alpha-1}{\alpha}\right)\cdot\left(\frac{k_2'}{1+k_2'}\right)\cdot\left(\frac{1-(t_0/t_m)}{1+(t_0/t_m)k_1'}\right) \quad (1)$$

where α is the separation factor, i.e. selectivity; N is the number of theoretical plates; k_2' and k_1' are the capacity factors of solutes 1 and 2 and t_0 and t_m are the migration times of EOF and micellar phase, respectively. In the RM-MEKC mode, electroosmotic flow (t_0) is virtually eliminated by applying a coated capillary; as a consequence of minimal t_0, resolution can be expressed as [8]:

$$R_{s_{\text{RM-MEKC}}} = \frac{\sqrt{N}}{4}\cdot\left(\frac{\alpha-1}{\alpha}\right)\cdot\left(\frac{k_2'}{1+k_2'}\right) \quad (2)$$

In addition to the difference in resolutions in the N-MEKC (Eq. (1)) and the RM-MEKC (Eq. (2)), the retention behaviors in RM-MEKC could be different from the N-MEKC due to a zero EOF and a reversed high voltage applied. Therefore, an evaluation of the two separation modes by means of chemometric experimental designs and modeling would be of interest.

3.1. Experimental design and optimization

A CCD [22,23] (bar distance = 1.682) was utilized for the optimization of three factors in both N-MEKC and RM-MEKC. Two pairs of resolution, separation efficiency and migration times were set as responses, Tables 1 and 2. In total, 19 experiments including 5 central points were performed. For experiment number 11, a negative value for SDS was generated from the design, however, a value 10, which is above the SDS critical micellar concentration (CMC), was selected. Optimal values for three factors from the MLR modeling are presented in Table 3. All regression coefficients are given as 95% confidence.

3.2. Modeling from the MLR in N-MEKC and RM-MEKC

In modeling the N-MEKC separation, the MLR analysis identified 2 sets of data from experiments 10 and 13 as outliers and these were therefore excluded from the model. In modeling RM-MEKC, the data from 4 experiments (3, 9, 10 and 13) were excluded from the model. Table 3 gives the optimal values and regression coefficients for corresponding responses in two separation modes obtained from the MLR modeling. Good correlations between the models and data were obtained (most regression coefficient's squares >0.93, see R^2 and Q^2 in Table 3), indicating excellent models and model predictions as well. In one case low value ($Q^2 = 0.3211$) for Rs1 was observed. This implies a low prediction reliability of the model for the resolution of Ala and Gly in the RM-MEKC separation mode. In fact, this pair was not baseline resolved in some of the conditions examined. Table 3 shows that optimal BGE and SDS concentrations for resolutions and separation efficiencies were similar in N-MEKC and RM-MEKC modes (Rs1 is not reliable as mentioned above). However, a large difference in optimal BGE concentration for migration time was observed; for example, a low value of BGE concentration (12.1 m*M*) was required in the N-MEKC separation of Ala, but a high BGE concentration (60 m*M*) was needed for Ala in the RM-MEKC mode.

Table 1
Experiments and data from a central composite design for N-MEKC[a]

Factors				Responses					
Name	Buffer	SDS	HV	Rs1	Rs2	*N*-Asp $\times 10^5$	*N*-Ala $\times 10^5$	Time-Asp (min)	Time-Ala (min)
Low	20	10	15						
High	60	40	25						
Exp01	20	10	15	0.33	0.81	0.089	0.19	7.226	5.410
Exp02	60	10	15	1.11	2.11	0.96	0.35	8.867	6.562
Exp03	20	40	15	1.61	0.95	0.13	0.73	8.547	7.363
Exp04	60	40	15	2.63	2.50	1.00	1.40	9.873	8.755
Exp05	20	10	25	0.20	0.83	0.087	0.039	4.330	3.235
Exp06	60	10	25	1.09	1.90	0.94	0.42	5.103	3.782
Exp07	20	40	25	1.42	0.91	0.13	0.62	4.914	4.250
Exp08	60	40	25	2.35	2.51	1.02	1.35	5.606	4.942
Exp09	6.36	25	20	0.59	0.20	0.20	0.11	5.700	4.468
Exp10	73.64	25	20	2.17	2.79	1.26	1.09	7.177	5.840
Exp11	40	10	20	0.75	1.23	0.34	0.26	5.943	4.443
Exp12	40	50.23	20	2.23	2.02	0.42	1.22	6.977	6.460
Exp13	40	25	11.59	1.48	1.45	0.38	0.52	11.179	9.075
Exp14	40	25	28.41	1.47	1.39	0.35	0.50	4.291	3.476
Exp15	40	25	20	1.50	1.38	0.35	0.50	6.268	5.106
Exp16	40	25	20	1.50	1.37	0.35	0.50	6.226	5.084
Exp17	40	25	20	1.52	1.38	0.34	0.51	6.263	5.190
Exp18	40	25	20	1.50	1.36	0.35	0.52	6.278	5.140
Exp19	40	25	20	1.50	1.36	0.33	0.51	6.262	5.080

[a] Rs1 = Resolution for Ala and Gly, Rs2 = resolution for Glu and Asp; *N*-Asp and *N*-Ala are the efficiencies for Asp and Ala; Time-Asp and Time-Ala are the migration times for the Asp (last eluted peak) and Ala (first eluted peak).

3.3. Different migration time behavior of N-MEKC and RM-MEKC

In N-MEKC an increase in buffer concentration leads to a decrease in EOF and thereby to increased migration times. In RM-MEKC, there is no EOF, and the BGE here only affects the analyte-micelle equilibria. In Fig. 1 it is shown that an increase in BGE concentration in RM-MEKC led to decreased migration times which was opposite to that obtained in N-MEKC. The different migration behaviors are also illustrated from the modeling as a function of BGE and SDS concentrations in the N-MEKC and RM-MEKC modes, Fig. 2. The results strongly suggests that a low BGE concentration intended for a rapid separation in N-MEKC may not be applicable to a rapid separation in RM-MEKC. Conversely, a relatively high BGE concentration has to be applied in RM-MEKC in order to achieve short migration times.

The influence of SDS concentration also differs in the two modes. Normally, when the SDS concentration is increased, the analyte–micelle equilibrium is shifted towards the micelle. In N-MEKC this leads to increased migration times and in RM-MEKC it leads to decreased migration times. Analyte–micelle interaction would thus be simply according to analyte hydrophobicity. However, interaction may be more complex when micelles and analytes have the same sign of charge. In the present work, micelles as well as analytes are anionic. Electrostatic repulsion is involved in the analyte–micelle interactions and it competes with the hydrophobicity mechanism. It should be noted that, due to the derivatization the analytes have a relatively high hydrophobicity. However, we found that an increase in SDS concentration led to increased migration time for Asp, which has a double charge, but the opposite was observed for Ala, which has a single charge, Fig. 2. This means that for Asp, complexation with SDS decrease with

Table 2
Experiments and data from a central composite design for RM-MEKC[a]

Factors				Responses					
Name	Buffer	SDS	HV	Rs1	Rs2	*N*-Asp $\times 10^5$	*N*-Ala $\times 10^5$	Time-Asp (min)	Time-Ala (min)
Low	20	10	15						
High	60	40	25						
Exp01	20	10	15	0	1.43	0.18	0.14	10.950	13.772
Exp02	60	10	15	0.73	3.16	1.25	0.51	10.280	17.558
Exp03	20	40	15	1.74	1.32	0.17	0.98	10.660	12.654
Exp04	60	40	15	4.51	3.70	1.25	1.32	13.140	15.975
Exp05	20	10	25	0.24	1.55	0.21	0.047	6.579	13.349
Exp06	60	10	25	1.49	2.80	0.63	0.46	6.214	10.599
Exp07	20	40	25	4.34	2.25	0.21	0.63	9.837	13.725
Exp08	60	40	25	4.30	3.96	1.29	1.13	7.954	9.978
Exp09	6.36	25	20	2.12	0.67	0.011	0.082	11.403	23.288
Exp10	73.64	25	20	4.47	3.86	1.60	1.21	8.725	11.957
Exp11	40	10	20	0	2.55	0.73	0.14	7.901	14.318
Exp12	40	50.23	20	4.27	3.55	0.73	1.02	11.369	13.444
Exp13	40	25	11.59	4.39	3.28	0.92	0.85	16.142	24.390
Exp14	40	25	28.41	3.93	3.00	0.69	0.58	6.607	10.452
Exp15	40	25	20	4.03	2.98	0.75	0.66	9.317	14.247
Exp16	40	25	20	4.02	2.96	0.74	0.66	9.317	14.217
Exp17	40	25	20	3.98	2.95	0.73	0.65	9.303	14.194
Exp18	40	25	20	3.99	2.94	0.73	0.66	9.315	14.210
Exp19	40	25	20	4.01	2.93	0.76	0.64	9.314	14.211

[a] Rs1 = Resolution for Ala and Gly, Rs2 = resolution for Glu and Asp; *N*-Asp and *N*-Ala are the efficiencies for Asp and Ala; Time-Asp and Time-Ala are the migration times for the Asp (first eluted peak) and Ala (last eluted peak).

Table 3
Optimal values and regression coefficients from MLR modeling[a]

Modes	Response	Optimal values			Regression coefficients	
		BGE (m*M*)	SDS (m*M*)	HV (kV)	R^2	Q^2
N-MEKC[b]	Rs1	60	50	15	0.9905	0.9778
	Rs2	60	50	15	0.9958	0.9310
	N-Asp	60	50	25.8	0.9992	0.9981
	N-Ala	60	50	15	0.9918	0.8512
	Time-Asp	10	10.3	27	0.9996	0.9950
	Time-Ala	12.1	10	28	0.9993	0.9985
RM-MEKC[c]	Rs1	10	44.1	15	0.9892	0.3211
	Rs2	60	50	28	0.9986	0.9281
	N-Asp	60	50	28	0.9996	0.9982
	N-Ala	60	50	15	0.9974	0.8476
	Time-Asp	45.2	10	28	0.9990	0.9392
	Time-Ala	60	50	28	0.9999	0.9930

[a] Rs1 = Resolution for Ala and Gly, Rs2 = resolution for Glu and Asp; *N*-Asp and *N*-Ala are the efficiencies for Asp and Ala; Time-Asp and Time-Ala are the migration times for the Asp and Ala. R^2 is an overestimated and Q^2 underestimated measure of the goodness of fit of the model. Values close 1 for both R^2 and Q^2 indicate very good model with excellent predictive power. Separation conditions: Capillary 55 cm (47 cm to detector window) × 50 μm I.D. [b]uncoated capillary. [c]Coated capillary. Background electrolyte, boric acid–NaOH (pH 8.60).

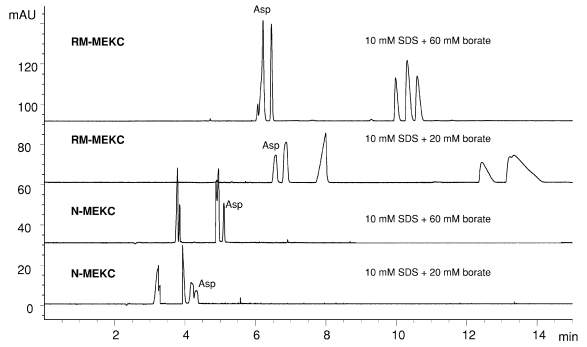

Fig. 1. Effects of background electrolyte on separation in N-MEKC and RM-MEKC. Sample, a neurotransmitter amino acid standard, derivatized with FMOC. Separation conditions, background electrolyte, boric acid–NaOH (pH 8.60), 10 m*M* SDS; capillary 55 cm (47 cm to detector window) ×50 μm I.D.; N-MEKC, uncoated capillary, +25 kV; RM-MEKC, coated capillary, −25 kV. Sample concentration, 200 μ*M*; injection; 50 mbar, 10 s. (Buffer composition, not optimized.)

increasing SDS concentration. It may be speculated that the two negatively charged groups counteract interaction with the micelles.

The MLR model also clearly shows the significant effects of each variable and their interactions on migration times in N-MEKC and RM-MEKC, Fig. 3. In N-MEKC mode, an increase in both buffer and SDS concentrations resulted in increased migration times, Fig. 3a,b. However, a variation of SDS concentration had stronger influences on migration times for the relatively more hydrophobic FMOC-Ala than for FMOC-Asp. In RM-MEKC, different effects of SDS on migration times for FMOC-Asp and FMOC-Ala were observed, Fig. 3c,d.

3.4. Resolution in N-MEKC and RM-MEKC

Tables 1 and 2 present experimental data for the central composite design. A comparison of the resolutions obtained for N-MEKC, Table 1, and RM-MEKC, Table 2, gives that, with a few exceptions, resolutions are higher in the RM-MEKC than in N-MEKC. This is in accordance with the conclusions in Ref. [8]. Further, when comparing the migration time differences, Δt_R, between Asp and Ala, Tables 1 and 2, it can be seen that Δt_R is always larger in the RM-MEKC than in the N-MEKC mode, indicating a wider elution window in RM-MEKC.

3.5. Reversal of migration elution order in RM-MEKC to facilitate impurity determination

A comparison of the separation of 5 neurotransmitter amino acids under optimal conditions is shown in Fig. 4. It should be noted that although the lower BGE concentration led to a rapid separation (decreased migration time) in N-MEKC as shown in Fig. 1, poor peak shapes and lower separation efficiencies especially for the resolution of Asp and Glu were observed at the lower BGE concentration. Therefore, a relatively high BGE concentration (60 m*M*) was applied in N-MEKC separation at the expense of relatively longer migration time. For the comparison of separations in N-MEKC and RM-MEKC, we used 40 m*M* SDS as optimal concentration when considering selectivity as well as migration time. As clearly shown in Fig. 4, a reversed elution order was obtained in the RM-MEKC mode. The reversal of peak elution order may facilitate peak identification and improve impurity determination in cases when the small peak of interest is eluted after a major one. This is illustrated in Fig. 5 where an improved impurity determination was obtained in RM-MEKC, Fig. 5c. The impurities in Fig. 5 were calculated by normalizing the impurity peak area to the sum of 5 major peak areas (each peak area divided by its corresponding migration time). Moreover, as shown in Fig. 5a and b in N-MEKC separation, an overloaded injection resulted in distorted peak shapes, such tailed peaks oftentimes occur when an uncoated capillary is being used. Separation efficiencies were similar in both separation modes, ranging from 2.5 to $3.2 \cdot 10^5$ theoretical plates per meter. RSDs for migration times (5 consecutive runs) were 0.32 and 0.063% in N-MEKC and RM-MEKC, respectively. In addition, an increase of about 80% UV absorbance was observed in the RM-MEKC separation under similar separation conditions and sample injection conditions. This is probably due to the fact that the use of a coated capillary minimized the adsorption of analytes at the capillary wall. Suitable sweeping conditions contributed to enhanced sensitivity. This is because the examined amino acids became relatively hydrophobic after derivatization with FMOC and they could therefore be subject to a sweeping-effect in the RM-MEKC mode on a coated capillary.

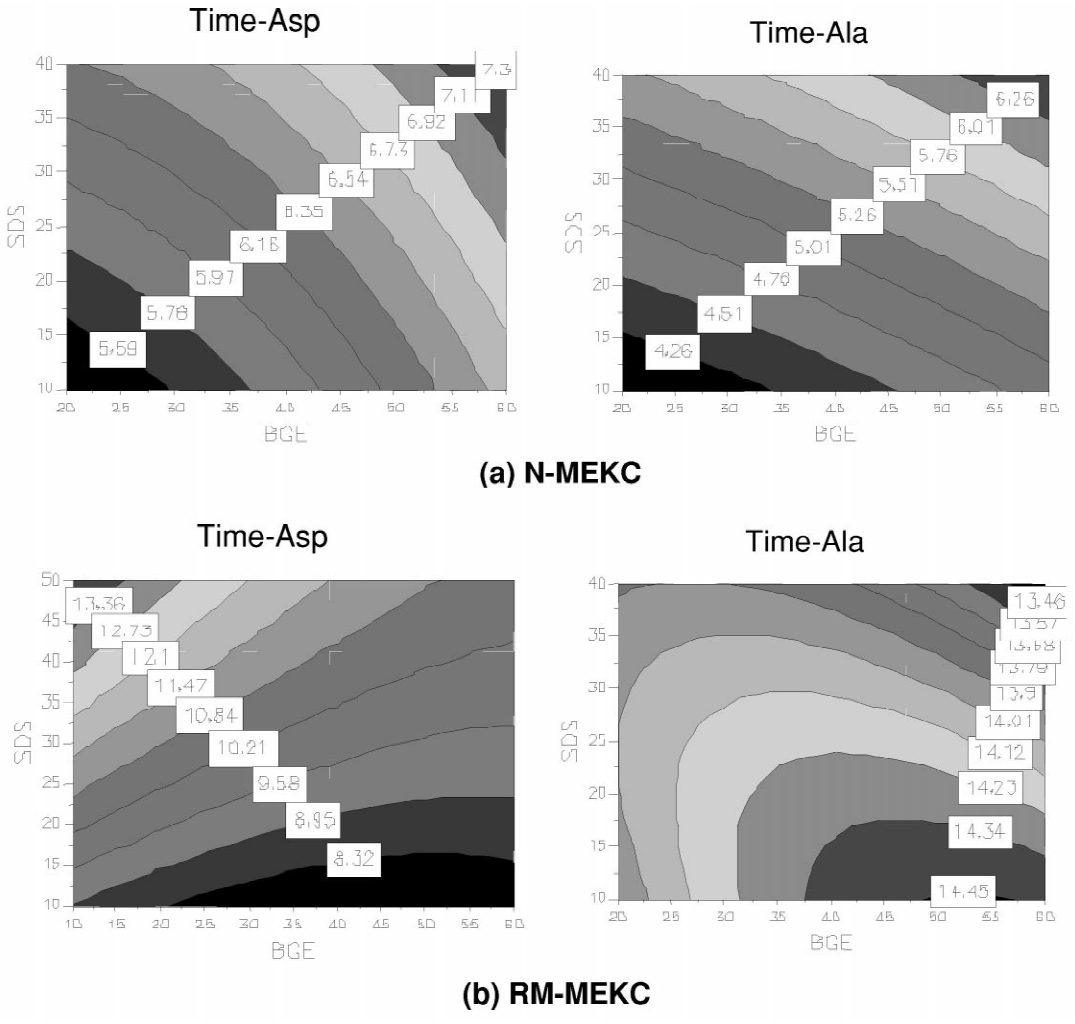

Fig. 2. Plots from simultaneous modeling of two factors, BGE and SDS. Sample, aspartic acid and alanine derivatized with FMOC. Separation conditions, background electrolyte, boric acid–NaOH (pH 8.60); capillary 55 cm (47 cm to detector window)×50 μm I.D., (a) coated capillary, −20 kV (b) uncoated capillary, +20 kV. Units: time (min), BGE (m*M*), SDS (m*M*). Time-Asp and Time-Ala are migration times for Asp and Ala.

The potential of increasing sensitivity using the sweeping technique by injecting a large sample volume was not further investigated as we intended mainly to compare two separation modes and their migration behaviors in this work.

4. Conclusions

The different retention behaviors of RM-MEKC and N-MEKC can be adequately described by a chemometric experimental design. In the present study we used a high pH BGE buffer for the resolution of neurotransmitter amino acids. Simultaneous separations of 5 primary neurotransmitter amino acids were achieved under optimized conditions in both separation modes. Optimal conditions regarding resolution and number of theoretical plates resulting from the optimization and modeling were quite similar for the N-MEKC and RM-MEKC

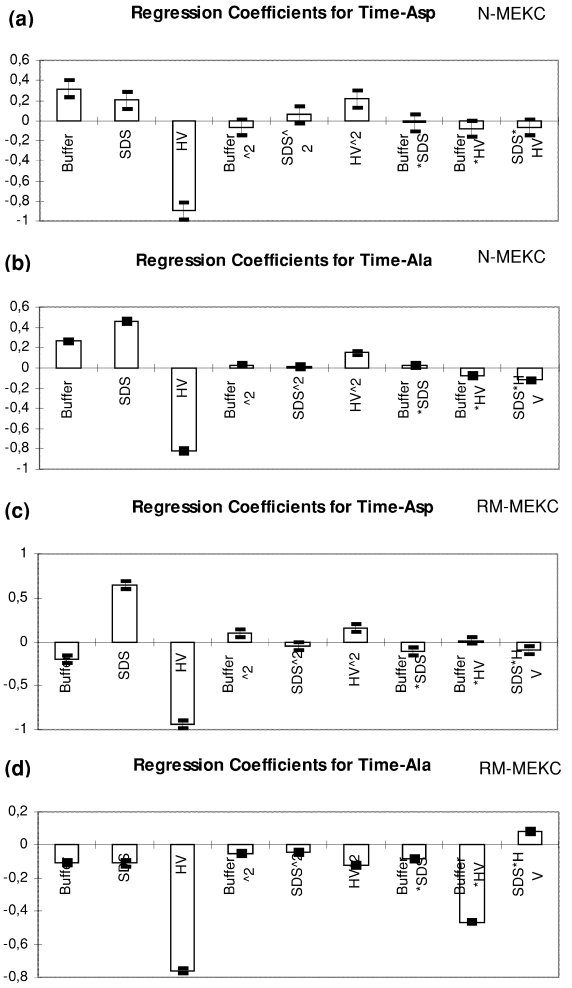

Fig. 3. Bar charts for the percentage main effects and interaction effects of the three main variables for the migration time in N-MEKC, (a) and (b), and RM-MEKC, (c) and (d), of aspartic acid and alanine derivatized with FMOC. Separation conditions as in Table 1.

modes. Optimal buffer composition regarding migration time was different, however.

To switch from one mode to the other can be rewarding. For example, in cases when an impurity peak is eluted right after a major peak in one of the two modes, the other mode will offer a reversed elution order, which most often leads to improved separation. This problem is often encountered in connection with impurity determinations in overloaded systems [35]. Thus, a combination of N-MEKC and RM-MEKC can be quite powerful since

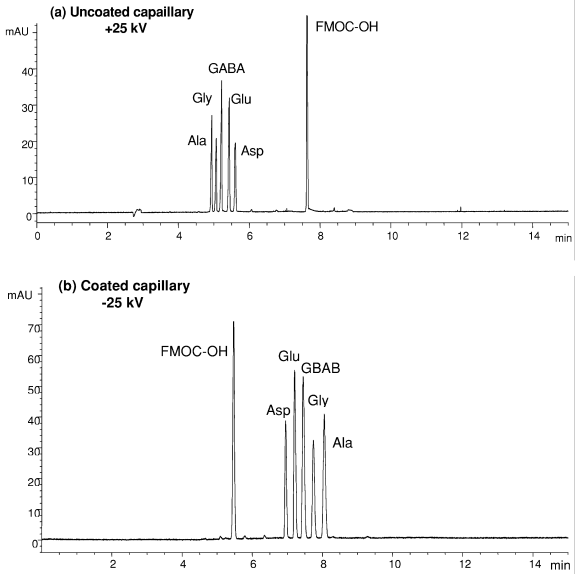

Fig. 4. Comparison of separation of 5 FMOC derivatized neurotransmitter amino acids in N-MEKC and RM-MEKC with reversed migration elution order. Sample, a neurotransmitter amino acid standard. Separation conditions, background electrolyte, 60 m*M* boric acid–NaOH (pH 8.60), 40 m*M* SDS; capillary 55 cm (47 cm to detector window)×50 μm I.D., (a) uncoated capillary, +25 kV, 24 μA; (b) coated capillary, −25 kV, 24 μA. Sample concentration, 200 μ*M*; injection; 50 mbar, 10 s.

the modes are complementary and this can be used for peak validation in quantitative analysis. However, the RM-MEKC mode provides some advantages that the N-MEKC mode does not. First, RM-MEKC separation in a coated capillary produces relatively symmetrical peaks and that is an advantage in quantitative analysis. Second, RM-MEKC approach gives better repeatability of migration times since the effect of EOF on migration times is negligible. Third, detection sensitivity can be somewhat enhanced as a consequence of the reduced adsorption of analytes at the coated capillary wall. A further advantage of RM-MEKC, as shown by Quirino and Terabe [8], is the improved stacking or sweeping effect for sensitivity enhancement for neutral and hydrophobic compounds as compared to stacking in N-MEKC mode. In our opinion, the reversed migration MEKC approach makes the MEKC technique particularly attractive. The application of RM-MEKC to other types of samples will be reported in a future paper.

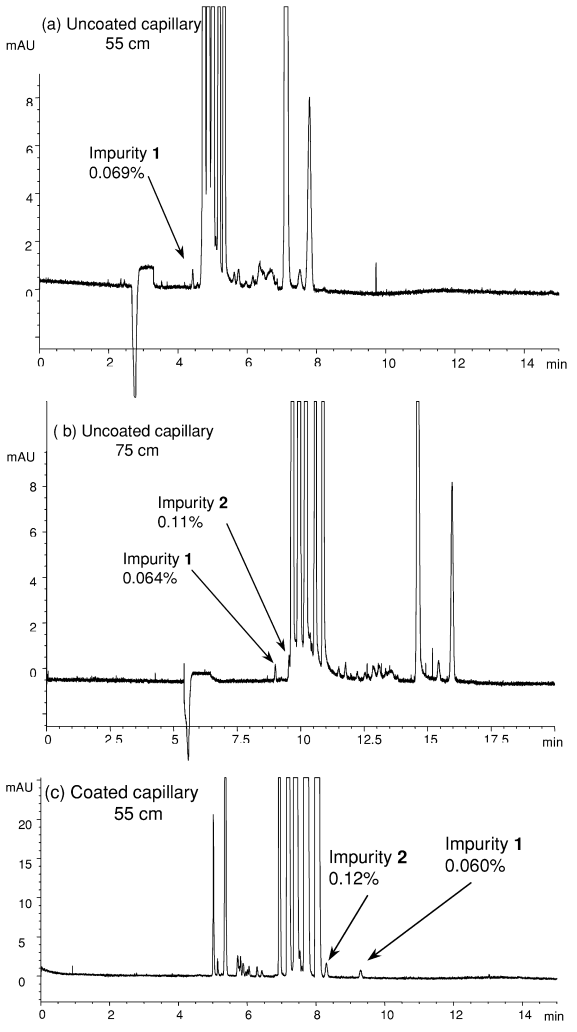

Fig. 5. Impurity profile from N-MEKC (uncoated capillary) and RM-MEKC (coated capillary). Sample, a neurotransmitter amino acid standard, FMOC derivatized. Separation conditions, background electrolyte, 60 m*M* boric acid–NaOH (pH 8.60), 40 m*M* SDS. (a) uncoated capillary 55 cm (47 cm to detector window)×50 μm I.D., 25 kV, 24 μA; (b) uncoated capillary 75 cm (67 cm to detector window)×50 μm I.D., 25 kV, 17 μA; (c) coated capillary 55 cm (47 cm to detector window)×50 μm I.D., −25 kV, 24 μA. Sample concentration, 1 mM; injection; 50 mbar, 10 s.

References

[1] J.P. Quirino, S. Terabe, J. Chromatogr. A 791 (1997) 119.
[2] J.P. Quirino, S. Terabe, J. Chromatogr. A 791 (1997) 255.
[3] J.P. Quirino, S. Terabe, Science 282 (1998) 465.
[4] J.P. Quirino, S. Terabe, J. Chromatogr. A 714 (1998) 29.
[5] J.P. Quirino, S. Terabe, Anal. Chem. 70 (1998) 149.
[6] J.P. Quirino, S. Terabe, Anal. Chem. 70 (1998) 1893.
[7] J.P. Quirino, S. Terabe, Anal. Chem. 71 (1999) 1638.
[8] J.P. Quirino, S. Terabe, J. Chromatogr. A 856 (1999) 465.
[9] M. Chiari, M. Nesi, G. Ottolina, P.G. Righetti, J. Chromatogr. A 680 (1994) 571.
[10] M.A. Abubaker, M.G. Bissell, J.R. Petersen, J. Capillary Electrophor. 2 (1995) 105.
[11] G.M. Janini, G.M. Muschik, H.J. Issaq, J. High Resolut. Chromatogr. 18 (1995) 171.
[12] G.M. Janini, G.M. Muschik, H.J. Issaq, J. Chromatogr. B 683 (1996) 29.
[13] G.M. Janini, G.M. Muschik, H.J. Issaq, Electrophoresis 17 (1996) 1575.
[14] G.M. Janini, H.J. Issaq, G.M. Muschik, J. Chromatogr. A 792 (1997) 125.
[15] A.M. Siouffi, R. Phan-Tan-Luu, J. Chromatogr. A 892 (2000) 75.
[16] C. Perrin, M.G. Vargas, Y. Vander Heyden, M. Maftouh, D.L. Massart, J. Chromatogr. A 883 (2000) 249.
[17] J. Havel, E.M. Pena, A. Rojas-Hernández, J.-P. Doucet, A. Panaye, J. Chromatogr. A 793 (1998) 317.
[18] J. Havel, M. Breadmore, M. Macka, P.R. Haddad, J. Chromatogr. A 850 (1999) 345.
[19] H. Corstjens, H.A.H. Billiet, J. Frank, K.Ch.A.M. Luyben, J. Chromatogr. A 715 (1995) 1.
[20] H. Corstjens, H.A.H. Billiet, J. Frank, K.Ch.A.M. Luyben, J. Chromatogr. A 753 (1996) 121.
[21] K.D. Altria, B.J. Clark, S.D. Filbey, M.A. Kelly, D.R. Rudd, Electrophoresis 16 (1995) 2143.
[22] H. Wan, L.G. Blomberg, J. Chromatogr. A 875 (2000) 43.
[23] R. Carlson, Design and Optimization in Organic Synthesis, Elsevier, Amsterdam, 1992.
[24] L. Eriksson, E. Johansson, N. Kettaneh-Wold, C. Wikström, S. Wold, Design of Experiments — Principles and Applications, Umetrics Academy, Umeå, Sweden, 2000.
[25] P.L. Weber, T.J. O'Shea, S.M. Lunte, J. Pharm. Biomed. Anal. 12 (1994) 319.
[26] S.Y. Zhou, H. Zuo, J.F. Stobaugh, C.E. Lunte, S.M. Lunte, Anal. Chem. 67 (1995) 594.
[27] J. Bergquist, M.J. Vona, C.O. Stiller, W.T. O'Connor, T. Falkenberg, R. Ekman, J. Neurosci. Methods 65 (1996) 33.
[28] C. Rocher, L. Bert, F. Robert, J.H. Trouvin, B. Renaud, C. Jacquot, A.M. Gardier, Brain Res. 737 (1996) 221.
[29] M.W. Lada, T.W. Vickroy, R.T. Kennedy, Anal. Chem. 69 (1997) 4560.
[30] Y. Zhang, B. Huang, J.K. Cheng, Anal. Chim. Acta 363 (1998) 157.
[31] P. Rada, S. Tucci, L. Teneud, X. Paez, J. Perez, G. Alba, Y. Garcia, S. Sacchettoni, J. del Corral, L. Hernandez, J. Chromatogr. B 735 (1999) 1.
[32] H. Wan, M. Öhman, L.G. Blomberg, in preparation.
[33] H. Wan, P.E. Andersson, A. Engström, L.G. Blomberg, J. Chromatogr. A 704 (1995) 179.
[34] S. Terabe, K. Otsuka, K. Ichikawa, A. Tsuchiya, T. Ando, Anal. Chem. 56 (1984) 111.
[35] L.G. Blomberg, H. Wan, Electrophoresis 21 (2000) 1940.